

Spatial scaling of extinction rates: Theory and data reveal nonlinearity and a major upscaling and downscaling challenge

Petr Keil¹  | Henrique M. Pereira^{1,2,3} | Juliano S. Cabral^{1,4} |

Jonathan M. Chase^{1,5} | Felix May¹ | Inês S. Martins¹ | Marten Winter¹

¹German Centre for Integrative Biodiversity Research (iDiv), Halle-Jena-Leipzig, Leipzig, Germany

²Institute of Biology, Martin Luther University Halle-Wittenberg, Halle (Saale), Germany

³Cátedra Infraestruturas de Portugal-Biodiversidade, CIBIO/InBIO, Universidade do Porto, Campus Agrário de Vairão, Vairão, Portugal

⁴Ecosystem Modeling, Center for Computational and Theoretical Biology (CCTB), University of Würzburg, Würzburg, Germany

⁵Institute of Computer Science, Martin-Luther University Halle-Wittenberg, Halle (Saale), Germany

Correspondence

Petr Keil, German Centre for Integrative Biodiversity Research (iDiv) Halle-Jena-Leipzig, Deutscher Platz 5e, 04103 Leipzig, Germany.
Email: pkeil@seznam.cz

Funding information

iDiv, Grant/Award Number: DFG FZT 118

Editor: Allen Hurlbert

Abstract

Aim: Biodiversity loss is a key component of biodiversity change and can impact ecosystem services. However, estimation of the loss has focused mostly on per-species extinction rates measured over a limited number of spatial scales, with little theory linking small-scale extirpations to global extinctions. Here, we provide such a link by introducing the relationship between area and the number of extinctions (number of extinctions–area relationship; NxAR) and between area and the proportion of extinct species (proportion of extinctions–area relationship; PxAR). Unlike static patterns, such as the species–area relationship, NxAR and PxAR represent spatial scaling of a dynamic process. We show theoretical and empirical forms of these relationships and we discuss their role in perception and estimation of the current extinction crisis.

Location: U.S.A., Europe, Czech Republic and Barro Colorado Island (Panama).

Time period: 1500–2009.

Major taxa studied: Vascular plants, birds, butterflies and trees.

Methods: We derived the expected forms of NxAR and PxAR from several theoretical frameworks, including the theory of island biogeography, neutral models and species–area relationships. We constructed NxAR and PxAR from five empirical datasets collected over a range of spatial and temporal scales.

Results: Although increasing PxAR is theoretically possible, empirical data generally support a decreasing PxAR; the proportion of extinct species decreases with area. In contrast, both theory and data revealed complex relationships between numbers of extinctions and area (NxAR), including nonlinear, unimodal and U-shaped relationships, depending on region, taxon and temporal scale.

Main conclusions: The wealth of forms of NxAR and PxAR explains why biodiversity change appears scale dependent. Furthermore, the complex scale dependence of NxAR and PxAR means that global extinctions indicate little about local extirpations, and vice versa. Hence, effort should be made to understand and report extinction rates as a scale-dependent problem. In this effort, estimation of scaling relationships such as NxAR and PxAR should be central.

KEYWORDS

Anthropocene, continental, grain, habitat loss, local, mass extinction, MAUP, metapopulation, patch, resolution

This is an open access article under the terms of the Creative Commons Attribution License, which permits use, distribution and reproduction in any medium, provided the original work is properly cited.

© 2017 The Authors. *Global Ecology and Biogeography* Published by John Wiley & Sons Ltd

1 | INTRODUCTION

Biodiversity loss is one of the most serious environmental problems we face (Cardinale et al., 2012; Pereira, Navarro, & Martins, 2012; Rockström et al., 2009), and estimates of its rate and magnitude are required for informed conservation policy. The Aichi target 12 under the Strategic Plan for Biodiversity 2011–2020 (www.cbd.int/sp/targets/) aims at preventing extinctions of known threatened species, and all regional and global assessments of Intergovernmental science-policy Platform on Biodiversity and Ecosystem Services (IPBES, <http://www.ipbes.net/>) are committed to report past, present and future trends of biodiversity. Given the importance of extinction rates to the process of biodiversity loss, it is striking that there are major unresolved issues related to spatial scale and metrics of extinctions.

Global extinction science has primarily focused on estimation of per-species extinction rates, measured as the number of extinctions per million species-years, E/MSY (e.g., Barnosky et al., 2011; Proenca & Pereira, 2013; Pimm et al., 2014). Similar per-species metrics have been used in island biogeography (e.g., Wu & Vankat, 1995) and metapopulation biology (Hanski, 1991), where they are termed per-species extinction rate or per-species extinction probability. All of these metrics are independent of the absolute number of species, which makes them comparable across epochs, regions and taxa. However, in addition to per-species rates, absolute counts of extinction events per unit of area are also of major interest, because they affect species richness, which is a core quantity of basic biodiversity science (Gaston, 2000), with links to ecosystem services (Cardinale et al., 2012; Hooper et al., 2005). Recently, a number of authors have been particularly interested in understanding how species richness changes through time, with debate as to whether it is declining at all scales or instead has more variable trends (Dornelas et al., 2014; Gonzalez et al., 2016; McGill, Dornelas, Gotelli, & Magurran, 2015; Vellend et al., 2013).

Spatial scale is a fundamental, but still mostly overlooked, aspect of understanding extinction. Current extinction rates have been estimated at global and continental extents (Alroy, 2015; Barnosky et al., 2011), which are crucial because they are irreversible. Yet, almost any global extinction is preceded by a series of local and regional extinctions (known as extirpations). For example, although the Danube clouded yellow (*Colias myrmidone*, Esper 1780) still survives in some parts of Europe, this butterfly was extirpated from the Czech Republic in 2006, which triggered considerable attention for its implications for landscape management across the whole continent (Konvicka et al., 2007). More prominent examples include extirpations of the bison [*Bison bison*, Linnaeus 1758 (Isenberg, 2001)] in most parts of North America, or lion [*Panthera leo*, Linnaeus 1758 (Riggio et al., 2013)] across most of Africa; local loss of these keystone species led to direct impacts on local ecosystem services. Clearly, focusing solely on global extinctions can underestimate extinctions on smaller scales, and vice versa; hence, there is a need to assess and understand the current extinction crisis at multiple spatial scales simultaneously.

Here, we propose a new way of looking at extinction rates to address the issues of metric and scale of extinction over continuous space. Specifically, we propose to consider jointly how numbers of

extinctions, N_X , and proportion of extinct species, P_X , scale with the area over which they are observed. We first provide theoretical expectations for the scaling of N_X and P_X . We then demonstrate the scaling using five empirical datasets covering local, regional and continental scales. We show that whereas P_X mostly decreases with area, N_X follows complex relationships with area. The key finding is that N_X in small areas can be lower, but also higher, than N_X in large areas, making it impossible to obtain the complete picture of the current extinction crisis from looking at a limited range of spatial scales (e.g., local or global).

2 | THE CONCEPT OF N_X AR AND P_X AR

Here, we establish two central concepts of this paper: (a) N_X AR, the relationship between number of extinction events, N_X , and the area of the observation window, A ; and (b) P_X AR, the relationship between the proportion of extinct species, P_X , and A , where $P_X = \frac{N_X}{S}$, and S is number of species in A at the beginning of a temporal interval (note that if $S=0$ then $N_X=0$ and P_X is undefined). In both cases, the area of the observation window is expanded in a nested way, so that a larger window always encompasses the smaller one. A window can be placed at any location within a larger continuous area and can overlap any number of habitat types (including uninhabitable areas). This makes P_X AR and N_X AR fundamentally different from approaches relating extinction probability to an area of a habitat patch (as in metapopulation ecology; Hanski & Ovaskainen, 2000) or to temporal change of habitat area (Kitzes & Harte, 2014). Furthermore, there are often multiple observation windows of the same (or similar) A representing cells of a grid (Figure 1a). In such cases, A becomes equivalent to the grid grain or resolution. When averaged over multiple grid cells or observation windows of a given A , N_X and P_X become \bar{N}_X and \bar{P}_X , and their scaling with A is \bar{N}_X AR and \bar{P}_X AR, which we use to summarize multiple realizations of N_X AR and P_X AR.

For the purpose of this paper, we classify an event as extinction when a species disappears from an observation window (i.e., present at time 1, but absent at time 2; Figure 1b). If the observation window is the entire world, such an event becomes a global extinction. When the species still prevails outside the observation window, an extinction event inside of the window can also be called an extirpation. Thus, at the global scale, N_X corresponds to the E metrics of Proenca and Pereira (2013) and Foote (1994), and our P_X corresponds to the $\frac{E}{S}$ metric of Proenca and Pereira (2013) and $\frac{E}{S}$ metric of Foote (1994). When observation windows are cells of a grid with a given grain A , we use $P(\text{ext}) = \frac{AOO_{\text{lost}}}{A_{\text{tot}}}$ (Supporting Information Appendix S1) for a single-species probability of extinction in a grid cell with a given A , where AOO_{lost} is the area of grid cells in which the species went extinct, and A_{tot} is the area of all grid cells in the entire studied region. Importantly, $\bar{N}_X = \sum_{i=1}^{S_{\text{tot}}} P(\text{ext})_i$ where S_{tot} is number of species in the entire region at time 1, and i identifies each species (Supporting Information Appendix S1). For details and connections between these metrics and/or links of P_X AR and N_X AR to scale–area curves (Hartley & Kunin, 2003; Kunin, 1998; Wilson, Thomas, Fox, Roy, & Kunin, 2004), see Supporting

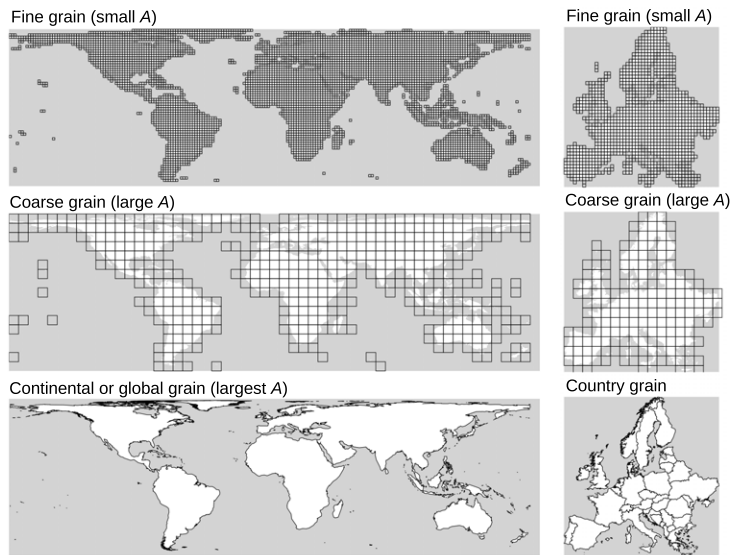
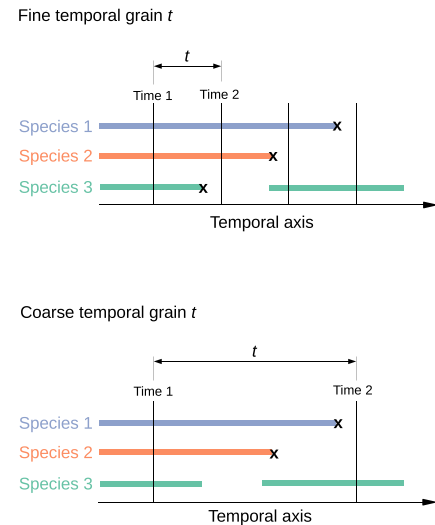
(a) - Spatial grain A (b) - Temporal grain (interval) t 

FIGURE 1 Extinctions and extirpations have spatial and temporal grain. (a) Our main focus is on extinction rates and numbers as a function of spatial grain, A (area of observation window), which can be a rectangular grid cell or an irregularly shaped country or continent. (b) Temporal grain (t) is the length of the interval between time 1 and time 2 over which extinction events (marked by x) are counted

Information Appendix S1. For a description of how P_{xAR} and N_{xAR} differ from endemics–area relationships (He & Hubbell, 2011; Keil, Storch, & Jetz, 2015) and extinction–area relationships (Kitzes & Harte, 2014), see Supporting Information Appendix S2.

Finally, we note that we can speak about extinction rates only after we express P_X and N_X (or their means, \bar{N}_X and \bar{P}_X) per unit of time, or temporal grain (the time interval t between time 1 and time 2; Figure 1b). Thus, the true rate metrics are N_X/t and P_X/t , where the latter corresponds to the widely used E/MSY (Barnosky et al., 2011; Pimm, Raven, Peterson, Şekercioğlu, & Ehrlich, 2006). However, with t , we face the non-trivial problem of temporal scaling. It has been shown that over paleontological time-scales, the means of both N_X and P_X typically increase nonlinearly with t (Foote, 1994), whereas the variance of P_X and N_X decreases with t (Alroy, 2014; Barnosky et al., 2011; Foote, 1994). The latter happens because extinction events tend to be clumped in time (Foote, 1994). Albeit important, we do not explicitly deal with temporal scaling in this paper. In most of our theoretical arguments and comparisons, we avoid the problem by assuming t is constant, and we focus on spatial scaling of N_X and P_X . In our empirical evaluations, we either report t alongside P_X and N_X , or we use N_X/t and P_X/t .

3 | THEORETICALLY EXPECTED SHAPES OF N_{xAR} AND P_{xAR}

We first show what not to expect. In Figure 2, we show that mean numbers of extinction events, \bar{N}_X , and the mean proportion of extinct species, \bar{P}_X , should not be expected to have a generally increasing or decreasing relationship with area. There are two scenarios that lead to different \bar{P}_{xAR} s and \bar{N}_{xAR} . (Figure 2a). In scenario 1, a region loses

two geographically restricted species, and nothing happens to the widespread species. This leads to \bar{N}_X being smaller at small grains than at larger grains, and both \bar{N}_{xAR} and \bar{P}_{xAR} are increasing. In scenario 2, there are range contractions of several widespread species, but no species is completely lost from the region. This results in high \bar{N}_X at small grains, but no extinctions at the larger grain. Here, \bar{N}_{xAR} and \bar{P}_{xAR} are decreasing (Figure 2a).

Using a minimalistic example of a single species in Figure 2b, we show that locally increasing, decreasing or hump-shaped relationships between A and single species $P(ext)$ are possible. This can happen, for example, when a peripheral fragment of a population is lost (see Supporting Information Appendices S1 and S3 for richer set of examples). We know that $\bar{N}_X = \sum_{i=1}^{S_{tot}} P(ext)_i$ (Supporting Information Appendix S1); hence, nonlinear relationships of $P(ext)_i$ with A can simply add up to nonlinear \bar{N}_{xAR} s. This confirms that \bar{N}_{xAR} s should exhibit a rich variety of functional forms, including decreasing, increasing and unimodal patterns. Unfortunately, this reasoning may not be applicable for predictions of nonlinear shape of \bar{P}_{xAR} , because we have failed to find a simple and direct link between per-grid cell extinction probability $P(ext)_i$ and the mean proportion of extinct species \bar{P}_X (see also Supporting Information Appendix S1).

We present yet another line of reasoning that leads to nonlinear N_{xAR} in Figure 3. Specifically, we show that P_{xAR} and N_{xAR} can be linked through species–area relationship (SAR), and that even when P_{xAR} is monotonically decreasing, the N_{xAR} can increase, decrease or be unimodal. In other words, even if the per-species rate of extinction is high locally but low regionally, the actual number of extirpations can be exactly the opposite. This is counterintuitive but easily validated. Let us assume that mean species richness S at time 1 follows a power-law SAR (Figure 3a) or any other monotonically increasing function.

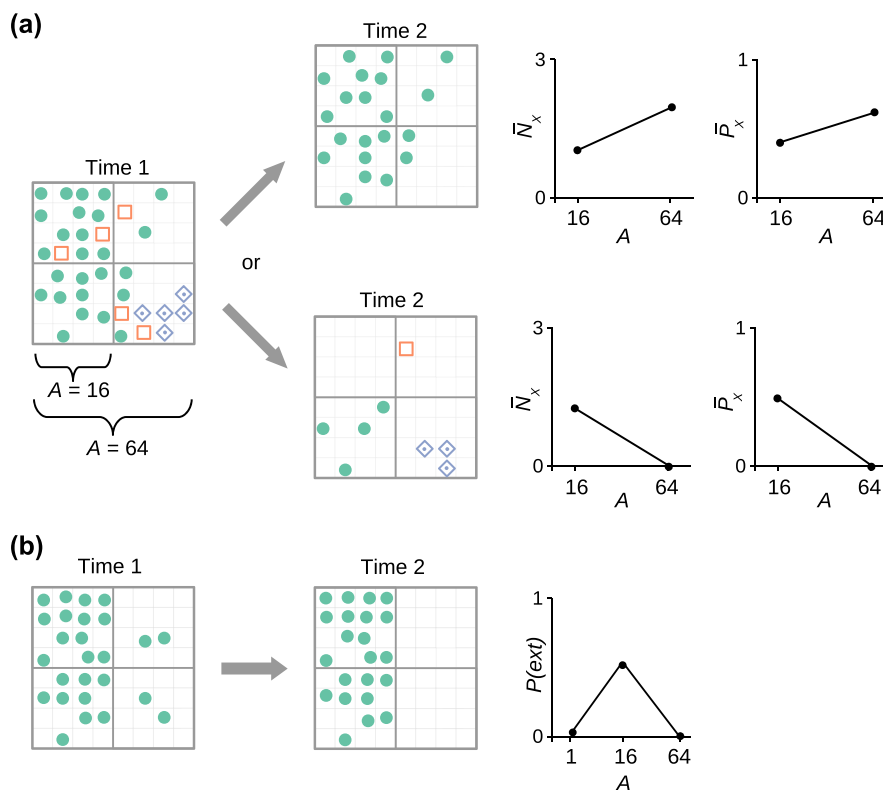


FIGURE 2 Simple scenarios showing the multitude of possible spatial scalings of extinction rates. (a) Two kinds of community dynamics producing opposite directions of \bar{N}_x AR and \bar{P}_x AR in a community that started with three species (indicated by symbol shape and colour) at time 1. In the first scenario, two rare species go extinct, leading to positive scaling. In the second scenario, none of the species goes completely extinct, but there are population declines in all species, leading to negative scaling. (b) Demonstration of the possibility of hump-shaped scaling of $P(\text{ext})$ with A . Notation: \bar{N}_x is the mean count of extinctions per grid cell of given spatial grain, A ; P_x is a mean per-grid cell P_x , where $P_x = \frac{N_x}{S}$, with S being number of species in a cell at time 1; and $P(\text{ext})$ is the proportion of grid cells that lost the species in the total number of grid cells

We move forward to time 2, assuming that each species at each location either goes extinct or survives. We can also assume that the P_x decreases with A monotonically, but with varying steepness (represented by different line types in Figure 3b). In such a system, N_x AR is obtained by multiplication of SAR with P_x AR; that is, at each grain, A , we take the number of species and multiply them by P_x to get N_x . As a result, the emerging shapes of N_x AR vary from increasing to hump shaped (Figure 3c), with the possibility of observing monotonically decreasing N_x AR over limited extents of A (Figure 3c).

The above SAR-based reasoning is general and applicable to any type of biodiversity dynamics, regardless of whether it is in equilibrium or not, and regardless of the mechanism causing the extinctions. However, in order to glimpse some mechanistic underpinnings of the extinction scaling, we also examined the shapes of P_x AR and N_x AR predicted by classical dynamic theories. First, we examined three variants of spatially implicit neutral models (Supporting Information Appendix S4): a closed local community dynamics with no immigration or speciation (Halley & Iwasa, 2011) a metacommunity model with random fission speciation and no local communities (Ricklefs, 2006), and a local community dynamics with immigration (Hubbell, 2001) (Supporting Information Appendix S4). These three variants predict increasing, decreasing or unimodal P_x ARs and N_x ARs, depending on how

migration is modelled, how time is scaled and whether we consider area of local community or area of a metacommunity (Supporting Information Appendix S4). Second, both metapopulation ecology (ME; Hanski, 2001; Hanski & Ovaskainen, 2000) and the equilibrium theory of island biogeography (ETIB; MacArthur & Wilson, 1967) assume a monotonically decreasing P_x AR, because larger patches or islands can host larger populations that are less likely to perish owing to environmental and demographic stochasticity (Lande, 1993). This is also supported empirically (Diamond, 1984; Hugueny, Movellan, & Belliard, 2011; Quinn & Hastings, 1987). In Supporting Information Appendix S5, we show that this decreasing P_x AR can be plugged into the ETIB to obtain increasing, decreasing or hump-shaped N_x AR, depending on how exactly immigration scales with area. However, note that ME and ETIB focus on areas of isolated habitat patches or islands of different sizes, without subdividing these to smaller spatial units; hence, we should not always generalize their predictions to mainlands, where area is a nested observational window.

To summarize, we have demonstrated that shapes of P_x AR and N_x AR are sensitive to whether widespread or rare species are affected by extinction, to whether peripheral or core parts of species distributions are lost, to the specific form of species–area relationship at time 1, to spatial scaling of immigration rates and to temporal grain. As a result,

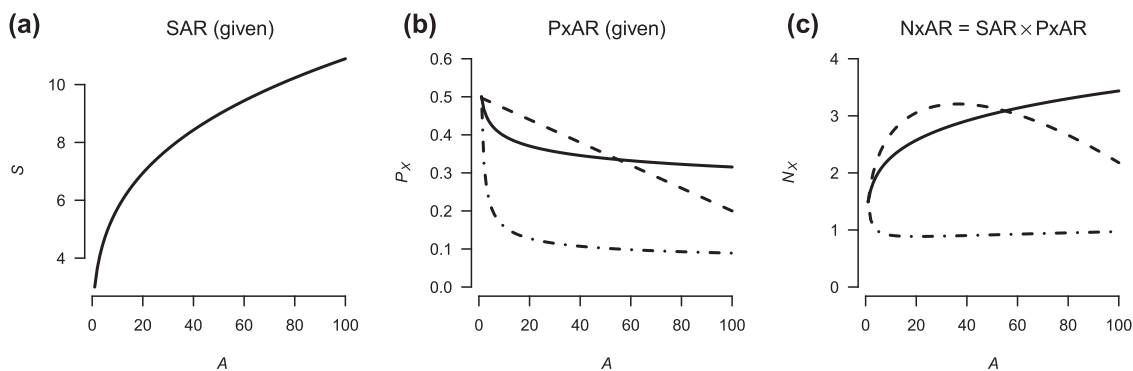


FIGURE 3 Spatial scaling of number of extinctions (N_X) derived from a simple species–area relationship (SAR)-based model. (a) SAR, the relationship between species richness S at time 1 and area A is given a priori; here it is a power law. (b) PxAR, the relationship between per-species extinction probability P_X and A , is also given a priori and is described by three arbitrarily selected monotonically decreasing functions. (c) By multiplying S by P_X at a given A , we get a rich variety of scalings of N_X , including monotonically decreasing, increasing or hump shaped. Dashing indicates corresponding PxAR and NxAR curves

both PxAR and NxAR can be increasing, nonlinear or decreasing. Such behaviour contrasts with ecological patterns such as nested species–area or endemics–area relationships that can only increase or remain flat.

4 | EMPIRICAL EVALUATION

We focused on mainland terrestrial systems with nested areas (continuous continental areas), mostly because of our own research background and because there is a well-developed literature on empirical extinction rates in island-like systems (Diamond, 1984; Hugueny et al., 2011; Quinn & Hastings, 1987; Tedesco et al., 2013).

4.1 | Data

We used the following five datasets that cover a wide range of geographical and temporal extents:

1. European butterflies. We extracted data on extinction events and on the extant species of butterflies (Lepidoptera: Rhopalocera) in European administrative areas during the last c. 100 years from Red data book of European butterflies (Van Swaay & Warren, 1999); specifically, we considered species extinct in a given country if its status in Van Swaay and Warren (1999) Appendix 6 table was 'Ex'.
2. European plants. We extracted the same kind of data on extinctions (between AD 1500 and 2009) and extant species of European vascular plants from Winter et al. (2009), available upon request from M.W. Note that the plant data cover different extent and administrative units from the butterfly data (Figure 4).
3. U.S. plants. We used data on the extant native species of *Plantae* (i.e., ferns, conifers and flowering plants) in 48 states of the U.S.A. (i.e., excluding Hawaii and Alaska) provided in the Biota of North America Program's (BONAP) North American Plant Atlas (Kartesz, 1999). We used data on contemporary (AD 1500–2009) extinction events also at the level of individual states. This information is provided by NatureServe (www.natureserve.org) and its network

of Natural Heritage member programmes (NatureServe, 2016). The data provided by NatureServe are for informational purposes, and should not be considered a definitive statement on the presence or absence of biological elements at any given location. Site-specific projects or activities should be reviewed for potential environmental impacts with appropriate regulatory agencies.

4. Czech birds. We used presence–absence data of breeding birds recorded in a regular grid of 11.7 km × 11.7 km grid cells throughout the Czech Republic, and covering two temporal periods: 1985–1989 (Štátný, Procházka, Bejček, & Hudec, 1997), with 56,780 species-per-cell incidences; and 2001–2003 (Štátný, Bejček, & Hudec, 2006), with 59,354 species-per-cell incidences. Hence, the temporal interval between the two periods is c. 14 years.
5. Barro Colorado trees. We used tree data from a 50-ha forest plot on Barro Colorado Island (BCI), Panama (Condit, 1998; Hubbell et al., 1999, 2005). For this analysis, we included only trees with ≥ 10 cm diameter at breast height (d.b.h.), and we compared two temporal snapshots 25 years apart. The results were qualitatively similar when the temporal lag between the two snapshots was 5, 10, 15 and 20 years, and also when we considered all trees with ≥ 1 cm d.b.h.

4.2 | NxAR and PxAR calculation

In the European, U.S. and Czech datasets, we constructed PxAR and NxAR curves by placing a small circle at a random location within the geographical extent of the data, then gradually increasing the circle size. For each circle size, we aggregated spatial units (i.e., European countries, U.S. states or Czech grid cells) overlapped by the circle. In the resulting aggregated units, we noted A , P_X , N_X and S , where A is the area of the aggregated unit, N_X the number of extinction events, S the number of all species found in the aggregated unit in the first temporal window, and $P_X = \frac{N_X}{S}$. This procedure was repeated 200 times, each time starting at a different random location of the smallest circle. We obtained a set of curves for each starting position, which we

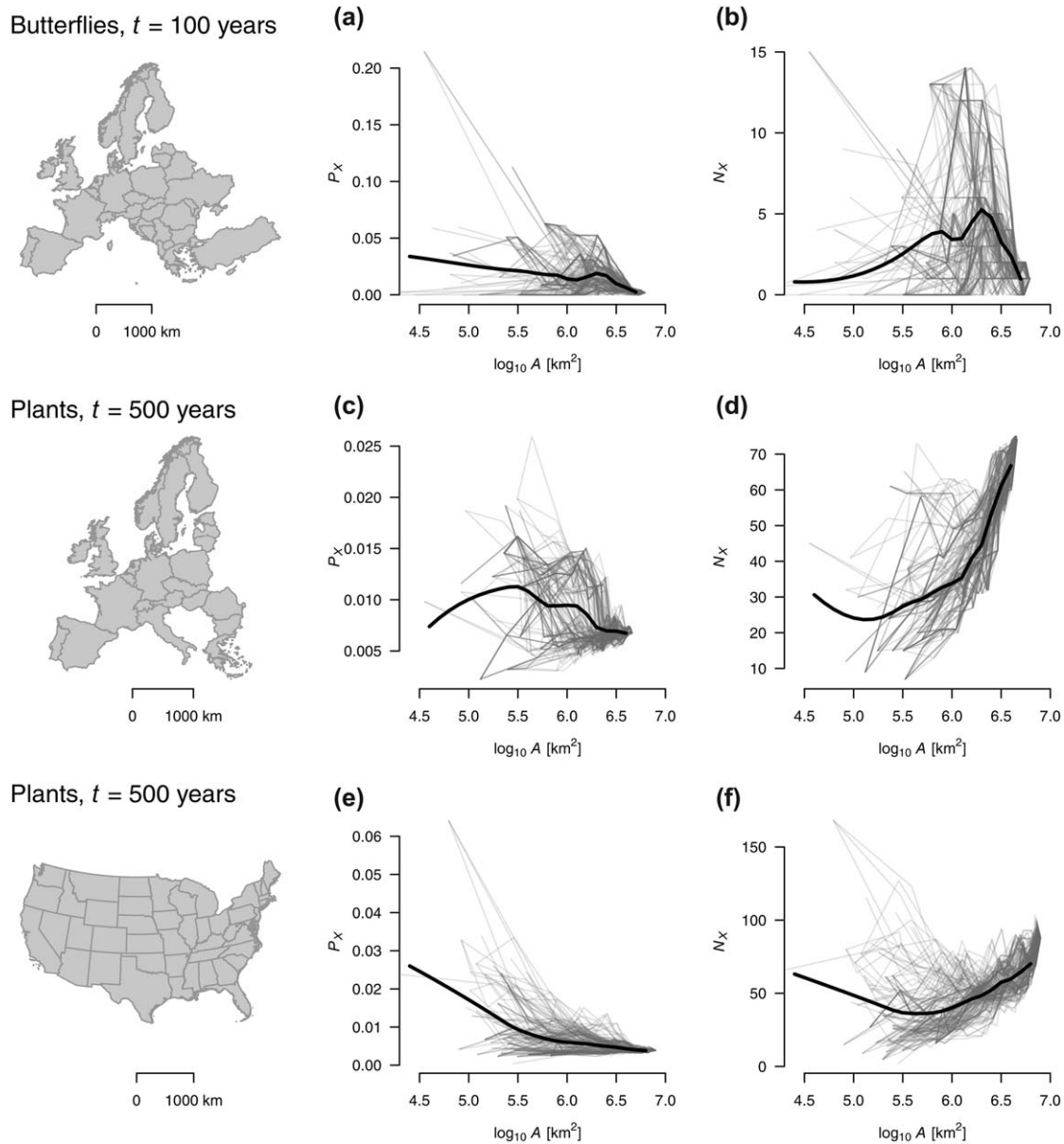


FIGURE 4 Empirical spatial scaling of (a, c, e) proportion of extinct species P_X and (b, d, f) number of extinctions N_X of (a, b) European butterflies, (c, d) European vascular plants and (e, f) U.S. vascular plants. Each grey line was obtained by placing (200 times) a small circle at a random location within the region, then gradually increasing the circle size up to the size of the whole region, counting the number of extinction events within the countries or states falling in the circle. Continuous black lines are LOESS regressions with a smoothing span of 0.3, and represent \bar{P}_X and \bar{N}_X

summarized using local regression (LOESS) with smoothing span of 0.3; the resulting smoothed average represents \bar{N}_X and \bar{P}_X . In the BCI forest plot, we overlaid the entire plot area with rectangular grids of increasing resolution, from 20 m \times 20 m up the entire 50 ha plot. At each grid resolution, we counted, for each grid cell, the number of species (S_0) in the 1985 census, checked which of these species were present in the 2010 census (S_1) and calculated $P_X = (S_0 - S_1) / S_0$ and $N_X = S_0 - S_1$. We then calculated average (\pm SD), \bar{N}_X and \bar{P}_X across all grid cells of a given grain.

Using the procedures described above, we obtained a smoothed average \bar{N}_X and \bar{P}_X for each A in each of the five datasets. However,

the datasets vary widely in their temporal grain, t . Hence, we also calculated spatial scaling of the \bar{P}_X/t and \bar{N}_X/t metrics derived from the smoothed averages, with t expressed as years between time 1 and 2. In case of the U.S. and European datasets, t is only a rough calculation, because the times of extinctions are not precisely known in most cases.

4.3 | Results

In the five empirical datasets, \bar{P}_X mostly decreases with area, A , of the observation window (Figures 4a,c,e and 5a,c). This contrasts with \bar{N}_X ,

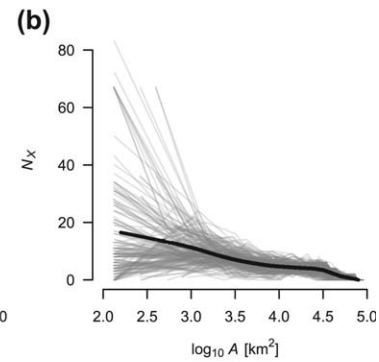
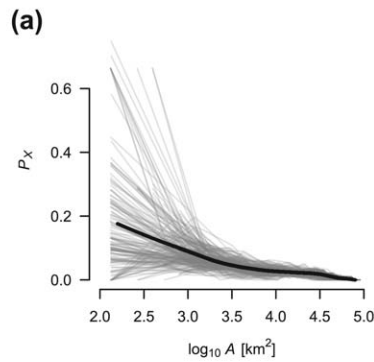
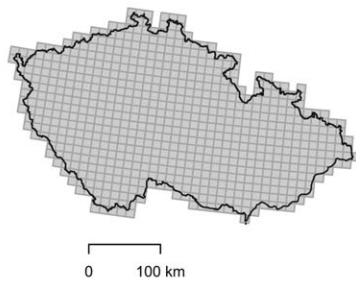
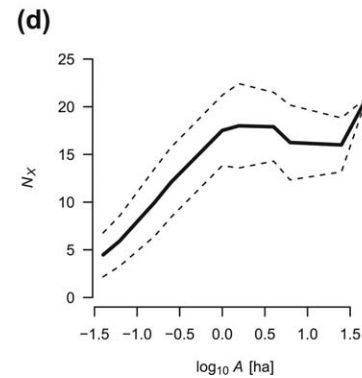
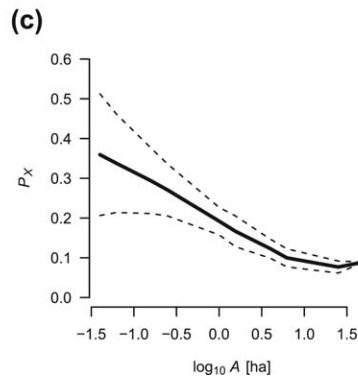
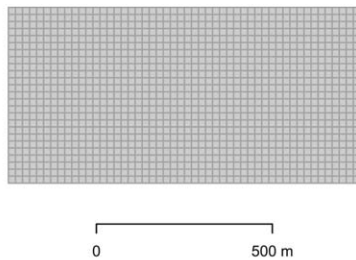
Birds, $t = 14$ yearsTrees, $t = 25$ years

FIGURE 5 Empirical spatial scaling of (a, c) proportion of extinct species P_X and (b, d) number of extinctions N_X in a country-wide and a local dataset. (a, b) Atlas data on birds of Czech Republic. Each grey line was obtained by placing (200 times) a small circle at a random location within the Czech Republic, then gradually increasing the circle size, counting numbers of extinctions in the atlas cells overlapping the circle. Continuous black lines are local regressions (LOESS, span = 0.3) and represent \bar{P}_X and \bar{N}_X . High values of P_X and N_X in some small areas are likely to be caused by undersampling. (c, d) Data on trees with diameter at breast height (d.b.h.) ≥ 10 cm in the 50-ha Barro Colorado Island (BCI) forest plot calculated over a 25-year lag. Continuous black lines are means and represent \bar{P}_X and \bar{N}_X , and dashed lines are standard deviations calculated over different spatial locations of the observation window

which scales with A in a variety of ways. The two datasets on European plants and butterflies produced highly divergent \bar{N}_X ARs (Figure 4b,d). European butterflies (Figure 4b) have a hump-shaped \bar{N}_X AR, with high numbers of extirpations at intermediate scales, but only a single pancontinental extinction. In contrast, European vascular plants (Figure 4d) have an upward-accelerating \bar{N}_X AR, with highest rates of extinction at the largest scale. The \bar{N}_X AR of the U.S. plants is similar to that of the European plants (Figure 4f), showing a clear upward acceleration at larger areas. In these continental datasets, we can explain the observed extinction scaling with range dynamics of rare and widespread species. The observed decrease of \bar{N}_X with A at large scales in European butterflies is likely to reflect range contractions, but not complete extinctions, of widespread species (e.g., as in Figure 2a). This is the opposite of the observed increase of \bar{N}_X with A at large scales in European and U.S. plants, which is more likely to reflect complete losses of small-ranged species (Figure 2a). Importantly, these disparate directions of \bar{N}_X AR are perfectly reconcilable with the decreasing \bar{P}_X AR in all of these datasets, as we have described in the SAR-based model (Figure 3).

We found decreasing \bar{N}_X AR in Czech birds (Figure 5b). Here, we note that the high values of N_X at small scales can be a result of under-sampled grid cells (see Section 4.4 below). On the even smaller scale of

the 50-ha BCI forest plot (Figure 5d), the \bar{N}_X AR sharply increases at the finest scale and is humped at larger scales, unveiling the possibility of multi-modal \bar{N}_X ARs. Our observations of decreasing \bar{P}_X AR and increasing \bar{N}_X AR at the local scale of the BCI plot are in line with predictions of the classical neutral model of Hubbell (2001) (Supporting Information Appendix S4). In both cases, \bar{N}_X approaches zero as A approaches zero, which stems from the trivial fact that the limited number of individuals in small areas can belong to only a limited number of species. Interestingly, as A increases and approaches the size of the BCI plot, both the neutral model and the empirical BCI data reveal a flat phase of the \bar{N}_X AR; we suggest that this is because the strong limiting effect of the small number of individuals no longer applies above a certain A .

When smoothed averages of \bar{P}_X , \bar{N}_X , \bar{P}_X/t and \bar{N}_X/t are simultaneously plotted as a function of A (Figure 6), no clear overall pattern emerges (or more precisely, our data are insufficient to reveal a clear pattern, if there is one). Figure 6 also shows that when t is considered (Figure 6c,d), the relative position of curves from different systems changes compared with raw \bar{P}_X AR and \bar{N}_X AR. What remains robust to the rescaling, however, are the high extinction rates in BCI trees and Czech birds, which are also datasets with the shortest t .

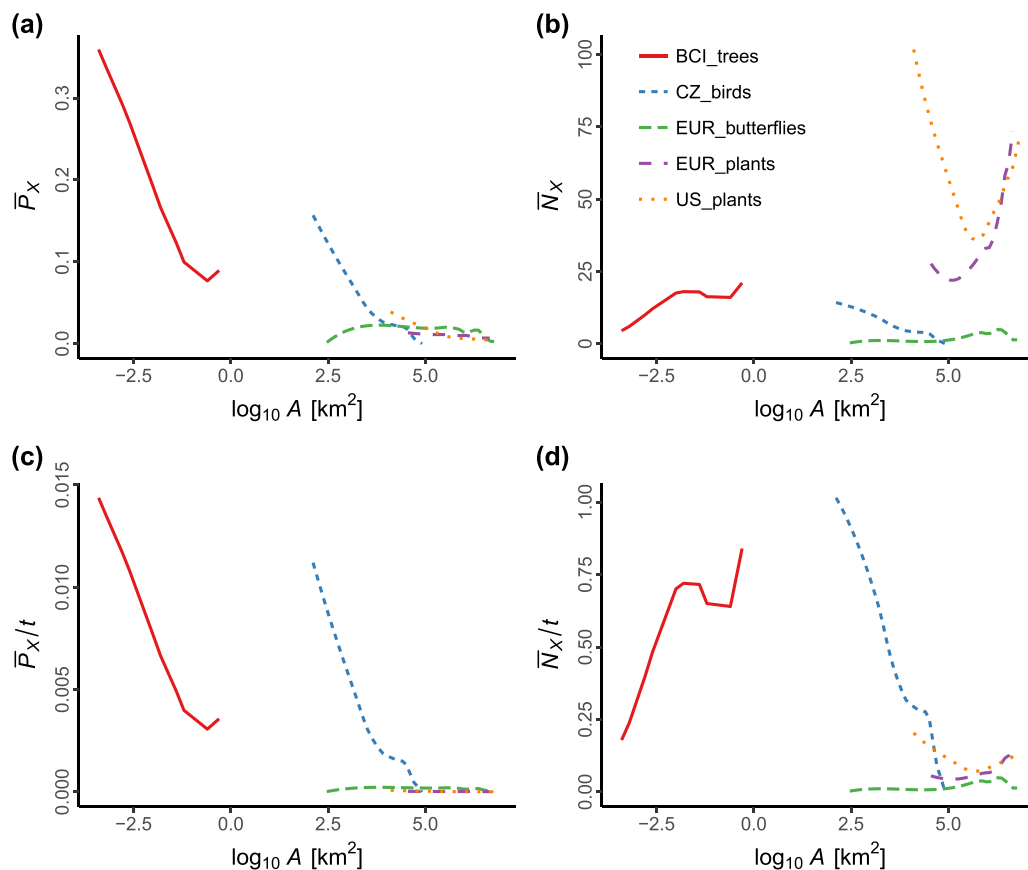


FIGURE 6 Empirical spatial scaling of means of four metrics of extinction rates derived from five datasets. The lines in (a) and (b) are smoothed averages extracted from Figures 4 and 5. In panels (c) and (d), the \bar{P}_X and \bar{N}_X are divided by the length of temporal interval t (in years), so that the rates represent \bar{P}_X/t or \bar{N}_X/t per year

4.4 | Limitations

Our selection of five empirical datasets revealed critical data limitations. First, we clearly need more empirical scaling curves from more scales, regions and taxa in order to be able to reject firmly or establish any empirical generality. Second, we should expect temporal survey data with continuous spatial coverage and grains between $1 \text{ km} \times 1 \text{ km}$ and $10 \text{ km} \times 10 \text{ km}$ to be rare (Beck et al., 2012; Jetz, McPherson, & Guralnick, 2012); we can already get a notion of this gap in Figure 6. Survey data from these grains also tend to suffer from false negatives (Hurlbert & Jetz, 2007), which can falsely elevate extinction rates. This may have generated the high extinction rates observed at the smallest grain of the Czech bird dataset. Here, we see an opportunity to extend imperfect detectability occupancy models (Kéry & Royle, 2015; Royle & Dorazio, 2008) to the problem of estimation of extinction rates. Third, species richness depends not only on area, but also on the shape of the area (Kunin, 1997). This might have added some noise to P_X and N_X calculated in irregularly shaped countries and states.

Finally, the effect of temporal grain t on extinction rates cannot be overstated (Figures 1b and 6c,d; Alroy, 2014; Barnosky et al., 2011; Foote, 1994). Although we have formulated our theoretical arguments to work for any t , our empirical datasets varied substantially in t . Moreover, datasets with the shortest t (BCI trees and Czech birds) also exhibited high per-species extinction rates (i.e., temporal and spatial

grains were collinear). We attempted to account for differences in t by using \bar{P}_X/t and \bar{N}_X/t , which revealed that BCI trees and Czech birds have disproportionately higher extinction rates than the continental datasets. This can be caused by rapid species temporal turnover at small spatial grains, or by issues of \bar{P}_X/t and \bar{N}_X/t standardizations, which assume a time-homogeneous extinction risk (Foote, 1994).

5 | DISCUSSION

5.1 | Extinction crisis as a grain-dependent problem

Our most important result is the set of counterexamples. Based on simple theoretical arguments and five empirical datasets, we should not expect extinction rates to follow a monotonic relationship with area of observational window (spatial and temporal grains). Instead, local rates can be similar, lower or higher than global rates. Thus, by solely focusing on global extinctions, we might miss either that not much is happening at small grains or that there are drastic losses at the small grains. Moreover, even nonlinear relationships are possible, with rates of species loss highest (concave curve) or lowest (convex curve) at intermediate grains. This complex behaviour is a warning to anyone reporting contemporary extinction rates (Alroy, 2015; Pimm & Raven, 2000; Pimm et al., 2006, 2014) or operating with terms such as ‘sixth mass extinction’ (Barnosky et al., 2011; Ceballos et al., 2015; Kolbert,

2014; Proenca & Pereira, 2013; Wake & Vredenburg, 2008). Our results reveal that these phenomena are grain dependent in a more pronounced and potentially less general way than static patterns of diversity. This is further complicated by the fact that per-species extinction rates and numbers of extinctions potentially differ in their relationship with area. For example, per-species extinction rate may decrease with area, whereas numbers of extinctions may increase with area in exactly the same taxon and region. Hence, any study reporting extinction rates at a single grain may fail to capture extinction dynamics fully by not considering those occurring at other grains. To provide a complete picture, local, regional and global extinctions should be estimated and reported simultaneously, preferably using multiple extinction metrics. The scaling curves we have developed offer a straightforward way to summarize and report multi-scale extinction rates.

5.2 | Upscaling, downscaling and interpolation of extinction rates

The nonlinear behaviour of PxAR and NxAR implies that a simple interpolation of extinction rates between grains should be done with caution, if at all. The same applies for an extrapolation of extinction rates at grains for which we have limited data (He & Hubbell, 2011; Pimm et al., 2014), the so-called upscaling and downscaling. Given the richness of possible NxAR shapes, we warn that estimating the magnitude of global extinction crisis from local species loss will be a major challenge. Likewise, numbers of local extinctions will be tricky to predict from global or continental extinction numbers. In both cases, we suggest that extra information is necessary on spatial scaling of the drivers of extinction (e.g., on spatial scaling of habitat dynamics or spatial scaling of intensity of extinction debts), on the specific distributions of species within the studied area and on their theoretical links to NxAR (e.g., as provided in Supporting Information Appendices S1 and S2).

An alternative approach could be to extrapolate PxAR, because it was mostly decreasing in our five datasets. If there is broad empirical support for an exact form of PxAR, then it should be possible to combine it with a species–area relationship (Figure 3) derived from the current global distributional information on some taxa [i.e., the International Union for Conservation of Nature (IUCN) range maps] to extrapolate extinction counts more reliably to grains that are coarser or finer than the grain of the extinction data. This can be a viable alternative to the recent approaches that predict extinction numbers solely from habitat loss (He & Hubbell, 2011; Keil, Storch, & Jetz, 2015; Martins & Pereira, 2017; Pereira & Daily, 2006; Pimm & Raven, 2000). Furthermore, a predictable PxAR can be instrumental in statistical models that link patterns of biodiversity with environmental drivers at multiple spatial scales (Keil & Jetz, 2013; Keil, Belmaker, Wilson, Unitt, & Jetz, 2013; McInerney & Purves, 2011).

5.3 | Grain-dependent biodiversity change

The uncovered wealth of possible relationships of extinction rates with area can also reconcile the reported lack of biodiversity change, on

average, at local grains (Dornelas et al., 2014; Vellend et al., 2013) with reported losses at the global extent (Alroy, 2015; Barnosky et al., 2011). The important lesson here is that there is no need to invoke species gains in order to explain a scale-dependent biodiversity loss, as suggested by Isbell et al. (2017); NxAR alone is sufficient to cause scale-dependent biodiversity dynamics (i.e., little change locally, but pronounced losses globally). However, we are also aware that for a complete picture of grain-dependent biodiversity change one also needs to know the spatial scaling of species gains (Jackson & Sax, 2010), and consequently, also species temporal turnover (combined losses and gains through time; McGill et al., 2015).

5.4 | Island versus mainland systems

We have shown that, in theory, per-species extinction rate can increase with area. How can a species be more likely to go extinct in a large area than in small one, given the classical view that larger areas host larger populations that are less susceptible to extinction (Diamond, 1984; Hanski, 2001; Lande, 1993; MacArthur & Wilson, 1967; Quinn & Hastings, 1987)? Our take is that the classical view is based on non-nested systems of islands or habitat patches, whereas here we operate over continuous 'mainland' areas with nested observational units [see Scheiner (2003) for treatment of the issue in the context of static SARs]. In nested systems, we can imagine a remote habitat patch or population occupying a small area at the periphery of a larger region (Figure 1b). Loss of such small populations can lead to complete extinction in the region, but may not contribute to the extinction rates in the majority of local communities. However, we note that in our empirical analyses, we still detected mostly decreasing PxARs, suggesting that it may be the prevalent form in mainland systems.

At the same time, we call for a more detailed theoretical and empirical comparison of the nested mainland and non-nested island systems. It is well known that island and mainland systems differ in their static scaling patterns of biodiversity (e.g., SARs), but the causes of such discrepancies remain controversial (Triantis, Guilhaumon, & Whittaker, 2012; Whittaker, Willis, & Field, 2001), and we suspect that it will be similarly challenging to explain fully the differences between island and mainland scalings of extinction rates.

5.5 | Outlook

Based on our results, we envision the following future research avenues:

1. To contribute to a more general agenda of dynamic macroecology, spatial scaling of extinctions should inspire a complementary approach focusing on scaling of species gains, which includes both immigration (invasion) and speciation.
2. Further theoretical insights into the scaling of extinctions can be obtained from spatially explicit neutral models (May, Huth, & Wiegand, 2015; Rosindell & Cornell, 2007) and from mechanistic simulation models (Cabral, Valente, & Hartig, 2017).

3. Spatial and temporal scaling of extinctions should be more closely integrated. Although paleontology has already seen theoretical and empirical evaluation of the role of t on global extinctions in the deep time (Alroy, 2014; Barnosky et al., 2011; Foote, 1994), we lack this at local grains and short t intervals. We suggest that survival analysis (Kleinbaum & Klein, 2005) could offer specific mathematical tools for short-term scaling of extinction rates.
4. More empirical datasets should be brought together to establish potential empirical generality of the scaling patterns. A grander task is then to estimate not only how fast species are lost at particular grains, but also where those losses occur. In other words, the grids that we introduced in Figure 1a should be populated with site- and scale-specific estimates of extinction rates.

ACKNOWLEDGMENTS

We are grateful to the handling editor Allen Hurlbert, to two anonymous referees and to A. Berger, C. Lawson and C. Meyer for helpful comments. The BCI forest dynamics research project was founded by S. P. Hubbell and R. B. Foster and is now managed by R. Condit, S. Lao and R. Perez under the Center for Tropical Forest Science and the Smithsonian tropical Research in Panama. Numerous organizations have provided funding, principally the U.S. National Science Foundation, and hundreds of field workers have contributed. All authors acknowledge funding of iDiv via the German Research Foundation (DFG FZT 118), while P.K., J.S.C. and M.W. acknowledge specifically funding through sDiv, the synthesis centre of iDiv.

DATA ACCESSIBILITY

A digitized form of the European butterfly data is available on Figshare at <https://doi.org/10.6084/m9.figshare.4036236.v1>. An electronic form of the Czech bird dataset is not publicly available; contact P.K. for details. Data on extant species of plants in U.S. states and European countries and on plant extinctions of European countries are also not publicly available; contact M.W. for details. Data on U.S. plant extinctions were purchased from NatureServe. The BCI data are available from CTFs through a request form (<http://ctfs.si.edu/webatlas/datasets/bci/>).

ORCID

Petr Keil  <http://orcid.org/0000-0003-3017-1858>

REFERENCES

- Alroy, J. (2014). Accurate and precise estimates of origination and extinction rates. *Paleobiology*, 40, 374–397.
- Alroy, J. (2015). Current extinction rates of reptiles and amphibians. *Proceedings of the National Academy of Sciences USA*, 112, 13003–13008.
- Barnosky, A. D., Matzke, N., Tomiya, S., Wogan, G. O. U., Swartz, B., Quental, T. B., ... Ferrer, E. A. (2011). Has the Earth's sixth mass extinction already arrived? *Nature*, 471, 51–57.
- Beck, J., Ballesteros-Mejia, L., Buchmann, C. M., Dengler, J., Fritz, S. A., Gruber, B., ... Dormann, C. F. (2012). What's on the horizon for macroecology? *Ecography*, 35, 673–683.
- Cabral, J. S., Valente, L., & Hartig, F. (2017). Mechanistic simulation models in macroecology and biogeography: State-of-art and prospects. *Ecography*, 40, 267–280.
- Cardinale, B. J., Duffy, J. E., Gonzalez, A., Hooper, D. U., Perrings, C., Venail, P., ... Naeem, S. (2012). Biodiversity loss and its impact on humanity. *Nature*, 486, 59–67.
- Ceballos, G., Ehrlich, P. R., Barnosky, A. D., Garcia, A., Pringle, R. M., & Palmer, T. M. (2015). Accelerated modern human-induced species losses: Entering the sixth mass extinction. *Science Advances*, 1, e1400253.
- Condit, R. (1998). *Tropical forest census plots*. Berlin, Germany: Springer.
- Diamond, J. M. (1984). "Normal" extinction of isolated populations. In M. H. Nitecki (Ed.), *Extinctions* (pp. 191–196). Chicago, IL: University of Chicago Press.
- Dornelas, M., Gotelli, N. J., McGill, B., Shimadzu, H., Moyes, F., Sievers, C., & Magurran, A. E. (2014). Assemblage time series reveal biodiversity change but not systematic loss. *Science*, 344, 296–299.
- Foote, M. (1994). Temporal variation in extinction risk and temporal scaling of extinction metrics. *Paleobiology*, 20, 424–444.
- Gaston, K. J. (2000). Global patterns in biodiversity. *Nature*, 405, 220–227.
- Gonzalez, A., Cardinale, B. J., Allington, G. R. H., Byrnes, J., Arthur Endsley, K., Brown, D. G., ... Loreau, M. (2016). Estimating local biodiversity change: A critique of papers claiming no net loss of local diversity. *Ecology*, 97, 1949–1960.
- Halley, J. M., & Iwasa, Y. (2011). Neutral theory as a predictor of avifaunal extinctions after habitat loss. *Proceedings of the National Academy of Sciences USA*, 108, 2316–2321.
- Hanski, I. (1991). Single-species metapopulation dynamics: Concepts, models and observations. *Biological Journal of the Linnean Society*, 42, 17–38.
- Hanski, I. (2001). Spatially realistic theory of metapopulation ecology. *Naturwissenschaften*, 88, 372–381.
- Hanski, I., & Ovaskainen, O. (2000). The metapopulation capacity of a fragmented landscape. *Nature*, 404, 755–758.
- Hartley, S., & Kunin, W. E. (2003). Scale dependency of rarity, extinction risk, and conservation priority. *Conservation Biology*, 17, 1559–1570.
- He, F., & Hubbell, S. P. (2011). Species–area relationships always overestimate extinction rates from habitat loss. *Nature*, 473, 368–371.
- Hooper, D. U., Chapin, F. S., Ewel, J. J., Hector, A., Inchausti, P., Lavorel, S., ... Wardle, D. A. (2005). Effects of biodiversity on ecosystem functioning: A consensus of current knowledge. *Ecological Monographs*, 75, 3–35.
- Hubbell, S. P. (2001). *The unified theory of biodiversity and biogeography*. Princeton, NJ: Princeton University Press.
- Hubbell, S. P., Condit, R., & Foster, R. B. (2005). *Barro Colorado forest census plot data*. Retrieved from <http://ctfs.si.edu/webatlas/datasets/bci>
- Hubbell, S. P., Foster, R. B., O'Brien, S. T., Harms, K. E., Condit, R., Wechsler, B., ... Loo de Lao, S. (1999). Light-gap disturbances, recruitment limitation, and tree diversity in a neotropical forest. *Science*, 285, 554–557.
- Hugueny, B., Movellan, A., & Belliard, J. (2011). Habitat fragmentation and extinction rates within freshwater fish communities: A faunal relaxation approach. *Global Ecology and Biogeography*, 20, 449–463.
- Hurlbert, A. H., & Jetz, W. (2007). Species richness, hotspots, and the scale dependence of range maps in ecology and conservation.

- Proceedings of the National Academy of Sciences USA*, 104, 13384–13389.
- Isbell, F., Gonzalez, A., Loreau, M., Cowles, J., Díaz, S., Hector, A., ... Larigauderie, A. (2017). Linking the influence and dependence of people on biodiversity across scales. *Nature*, 546, 65–72.
- Isenberg, A. C. (2001). *The destruction of the bison: An environmental history, 1750–1920*. Cambridge, U.K.: Cambridge University Press.
- Jackson, S. T., & Sax, D. F. (2010). Balancing biodiversity in a changing environment: Extinction debt, immigration credit and species turnover. *Trends in Ecology and Evolution*, 25, 153–160.
- Jetz, W., McPherson, J. M., & Guralnick, R. P. (2012). Integrating biodiversity distribution knowledge: Toward a global map of life. *Trends in Ecology and Evolution*, 27, 151–159.
- Kartesz, J. T. (1999). *A synonymized checklist and atlas with biological attributes for the vascular flora of the United States, Canada, and Greenland*. Chapel Hill, NC: North Carolina Botanical Garden.
- Keil, P., & Jetz, W. (2013). Downscaling the environmental associations and spatial patterns of species richness. *Ecological Applications*, 24, 823–831.
- Keil, P., Belmaker, J., Wilson, A. M., Unitt, P., & Jetz, W. (2013). Downscaling of species distribution models: A hierarchical approach. *Methods in Ecology and Evolution*, 4, 82–94.
- Keil, P., Storch, D., & Jetz, W. (2015). On the decline of biodiversity due to area loss. *Nature Communications*, 6, 8837.
- Kéry, M., & Royle, J. A. (2015). *Applied hierarchical modeling in ecology*. Cambridge, MA: Academic Press.
- Kitzes, J., & Harte, J. (2014). Beyond the species–area relationship: Improving macroecological extinction estimates. *Methods in Ecology and Evolution*, 5, 1–8.
- Kleinbaum, D. G., & Klein, M. (2005). *Survival analysis*. New York, NY: Springer.
- Kolbert, E. (2014). *The sixth extinction: An unnatural history*. New York, NY: Henry Holt & Company.
- Konvicka, M., Benes, J., Cizek, O., Kopecek, F., Konvicka, O., & Vitaz, L. (2007). How too much care kills species: Grassland reserves, agri-environmental schemes and extinction of *Colias myrmidone* (Lepidoptera: Pieridae) from its former stronghold. *Journal of Insect Conservation*, 12, 519–525.
- Kunin, W. E. (1997). Sample shape, spatial scale and species counts: Implications for reserve design. *Biological Conservation*, 82, 369–377.
- Kunin, W. E. (1998). Extrapolating species abundance across spatial scales. *Science*, 281, 1513–1515.
- Lande, R. (1993). Risks of population extinction from demographic and environmental stochasticity and random catastrophes. *The American Naturalist*, 142, 911–927.
- MacArthur, R. H., & Wilson, E. O. (1967). *The theory of island biogeography*. Princeton, NJ: Princeton University Press.
- Martins, I. S., & Pereira, H. M. (2017). Improving extinction projections across scales and habitat using the countryside species–area relationship. *Scientific Reports*, 7, 12899.
- May, F., Huth, A., & Wiegand, T. (2015). Moving beyond abundance distributions: Neutral theory and spatial patterns in a tropical forest. *Proceedings of the Royal Society B: Biological Sciences*, 282, 20141657.
- McGill, B. J., Dornelas, M., Gotelli, N. J., & Magurran, A. E. (2015). Fifteen forms of biodiversity trend in the Anthropocene. *Trends in Ecology and Evolution*, 30, 104–113.
- McInerney, G. J., & Purves, D. W. (2011). Fine-scale environmental variation in species distribution modelling: Regression dilution, latent variables and neighbourly advice. *Methods in Ecology and Evolution*, 2, 248–257.
- NatureServe (2016). *NatureServe central databases*. Arlington, VA: NatureServe.
- Pereira, H. M., & Daily, G. C. (2006). Modelling biodiversity dynamics in countryside landscapes. *Ecology*, 87, 1877–1885.
- Pereira, H. M., Navarro, L. M., & Martins, I. S. (2012). Global biodiversity change: The bad, the good, and the unknown. *Annual Review of Environment and Resources*, 37, 25–50.
- Pimm, S., Raven, P., Peterson, A., Şekercioğlu, Ç. H., & Ehrlich, P. R. (2006). Human impacts on the rates of recent, present, and future bird extinctions. *Proceedings of the National Academy of Sciences USA*, 103, 10941–10946.
- Pimm, S. L., & Raven, P. (2000). Biodiversity: Extinction by numbers. *Nature*, 403, 843–845.
- Pimm, S. L., Jenkins, C. N., Abell, R., Brooks, T. M., Gittleman, J. L., Joppa, L. N., ... Sexton, J. O. (2014). The biodiversity of species and their rates of extinction, distribution, and protection. *Science*, 344, 1246752.
- Proenca, V., & Pereira, H. M. (2013). Comparing extinction rates: Past, present, and future. *Encyclopedia of biodiversity*. In S. Levin (Ed.), *Encyclopedia of Biodiversity* (pp. 167–176). Cambridge, MA: Academic Press.
- Quinn, J. F., & Hastings, A. (1987). Extinction in subdivided habitats. *Conservation Biology*, 1, 198–208.
- Ricklefs, R. E. (2006). The unified neutral theory of biodiversity: Do the numbers add up? *Ecology*, 87, 1424–1431.
- Riggio, J., Jacobson, A., Dollar, L., Bauer, H., Becker, M., Dickman, A., ... Pimm, S. (2013). The size of savannah Africa: A lion's (*Panthera leo*) view. *Biodiversity and Conservation*, 22, 17–35.
- Rockström, J., Steffen, W., Noone, K., Persson, Å., Chapin, F. S., Lambin, E. F., ... Foley, J. A. (2009). A safe operating space for humanity. *Nature*, 461, 472–475.
- Rosindell, J., & Cornell, S. J. (2007). Species–area relationships from a spatially explicit neutral model in an infinite landscape. *Ecology Letters*, 10, 586–595.
- Royle, J. A., & Dorazio, R. M. (2008). *Hierarchical modelling and inference in ecology*. Cambridge, MA: Academic Press.
- Scheiner, S. M. (2003). Six types of species–area curves. *Global Ecology and Biogeography*, 12, 441–447.
- Štátný, K., Bejček, V., & Hudec, K. (2006). *Atlas hnízdního rozšíření ptáků v České republice, 2001–2003*. Prague, Czech Republic: Aventinum.
- Štátný, K., Procházka, P., Bejček, V., & Hudec, K. (1997). *Atlas hnízdního rozšíření ptáků v České republice, 1985–1989*. Jinočany, Czech Republic: H & H.
- Tedesco, P. A., Oberdorff, T., Cornu, J.-F., Beauchard, O., Brosse, S., Dürr, H. H., ... Hugueny, B. (2013). A scenario for impacts of water availability loss due to climate change on riverine fish extinction rates. *Journal of Applied Ecology*, 50, 1105–1115.
- Triantis, K. A., Guilhaumon, F., & Whittaker, R. J. (2012). The island species–area relationship: Biology and statistics. *Journal of Biogeography*, 39, 215–231.
- Van Swaay, C. A. M., & Warren, M. S. (1999). *Red data book of European butterflies*. Strasbourg, France: Council of Europe Publishing.
- Vellend, M., Baeten, L., Myers-Smith, I. H., Elmendorf, S. C., Beauséjour, R., Brown, C. D., ... Wipf, S. (2013). Global meta-analysis reveals no net change in local-scale plant biodiversity over time. *Proceedings of the National Academy of Sciences USA*, 110, 19456–19459.
- Wake, D. B., & Vredenburg, V. T. (2008). Are we in the midst of the sixth mass extinction? A view from the world of amphibians. *Proceedings of the National Academy of Sciences USA*, 105, 11466–11473.

- Whittaker, R. J., Willis, K. J., & Field, R. (2001). Scale and species richness: Towards a general, hierarchical theory of species diversity. *Journal of Biogeography*, 28, 453–470.
- Wilson, R. J., Thomas, C. D., Fox, R., Roy, D. B., & Kunin, W. E. (2004). Spatial patterns in species distributions reveal biodiversity change. *Nature*, 432, 393–396.
- Winter, M., Schweiger, O., Klotz, S., Nentwig, W., Andriopoulos, P., Ariannoutsou, M., . . . Kühn, I. (2009). Plant extinctions and introductions lead to phylogenetic and taxonomic homogenization of the European flora. *Proceedings of the National Academy of Sciences USA*, 106, 21721–21725.
- Wu, J., & Vankat, J. L. (1995). Island biogeography: Theory and application. In W. A. Nierenberg (Ed.), *Encyclopedia of Environmental Biology* (pp. 371–379). San Diego, CA: Academic Press.

BIOSKETCH

PETR KEIL is a synthesis postdoctoral researcher at sDiv, the synthesis centre of iDiv. His main interest is spatial scaling of multiple facets of biodiversity and its change. His hobby is statistics.

GERMAN CENTRE FOR INTEGRATIVE BIODIVERSITY RESEARCH (iDiv) is a research institute run by Martin Luther University Halle-Wittenberg (MLU), Friedrich Schiller University Jena (FSU) and Leipzig

University (UL), and in cooperation with the Helmholtz Centre for Environmental Research (UFZ). The goals of the institute, which was set up in 2012, are to record biological diversity in its complexity, to make available and use scientific data on a global level and to develop strategies, solutions and utilization concepts for decision-makers in order to prevent any further loss of biodiversity. iDiv promotes theory-driven synthesis, experiments and data-driven theory in biodiversity sciences and provides a scientific foundation for sustainable management of Earth's biodiversity.

SUPPORTING INFORMATION

Additional Supporting Information may be found online in the supporting information tab for this article.

How to cite this article: Keil P, Pereira HM, Cabral JS, et al. Spatial scaling of extinction rates: Theory and data reveal nonlinearity and a major upscaling and downscaling challenge. *Global Ecol Biogeogr.* 2018;27:2–13. <https://doi.org/10.1111/geb.12669>